from *P. vivax*, *P. falciparum*, *P. berghei*, *P. yoelii*, and *P. gallinaceum*. Reactivity to different strains of *P. vivax* (North Korean, Salvador 1, Colombian, and Thai) was also measured. The monoclonal antibody selected for passive transfer was designated NVS3 (Navy Vivax Sporozoite 3) and purified by affinity-column chromatography with staphylococcal protein A coupled to Sepharose 4B [H. Hjelm and J. Sjoquist, in *Immunoadsorbants in Protein Purification*, E. Ruoslahti, Ed. (University Park Press, Baltimore, MD, 1976), p. 51]. NVS3 was selected because it is species- and stage-specific and had the greatest activity in the IFAT against *P. vivax* sporozoites.

10. Sporozoites of the Salvador I strain were reared in *Anopheles stephensi* mosquitoes by membrane feeding the mosquitoes on gametocytemic chimpanzee blood [W. E. Collins, H. M. McClure, R. B. Swenson, P. C. Mehaffey, J. C. Skinner, *Am. J. Trop. Med. Hyg.* **35**, 56 (1986)]. Sixteen days after feeding, the sporozoites were dissected from the salivary glands of the infected mosquitoes for use in the challenge studies. On the basis of initial experiments, a dose of 2 mg of NVS3 per monkey was selected for injection intravenously into six *Saimiri* monkeys. An IgG3 monoclonal antibody directed against *Trypanosoma brucei rhodesiense* [T. Hall and K. Esser, *J. Immunol.* **132**, 2059 (1984)] was inoculated into another six monkeys to serve as an unrelated antibody control group. Nine other monkeys served as uninjected controls. One hour after antibody transfer, 10^4 *P. vivax* sporozoites in normal saline and 10% normal *Saimiri* monkey serum were injected into all monkeys. Serum samples were collected before antibody inoculation and 1 hour later (immediately before sporozoite challenge). All animals were splenectomized 6 to 7 days after sporozoite inoculation. Beginning 14 days after sporozoite inoculation and continuing through day 56, Giemsa-stained thick and thin blood films were prepared daily. Parasitemias were quantified and recorded per cubic millimeter of blood.
11. H. M. Geysen *et al.*, *Proc. Natl. Acad. Sci. U.S.A.* **81**, 3998 (1984); H. M. Geysen, S. J. Barteling, R. H. Meloen, *ibid.* **82**, 178 (1985); H. M. Geysen, S. J. Rodda, T. J. Mason, *Mol. Immunol.* **23**, 709 (1986); H. M. Geysen *et al.*, *J. Immunol. Methods* **102**, 259 (1987).
12. D. E. Arnot *et al.*, *Science* **230**, 815 (1985).
13. T. F. McCutchan *et al.*, *ibid.*, p. 1381.
14. D. E. Arnot, J. W. Barnwell, M. J. Stewart, *Proc. Natl. Acad. Sci. U.S.A.* **85**, 8102 (1988).
15. R. Rosenberg *et al.*, *Science* **245**, 973 (1989).
16. The eight-residue peptide $(AGDR)_2$ was synthesized by the stepwise solid-phase method [R. B. Merrifield, *J. Am. Chem. Soc.* **85**, 2149 (1963)]. Pam-*t*-Boc-L-arginine (Tos) resin (0.5 nmol) was used as the starting point of the synthesis. The protected peptide resin was deprotected by hydrogen fluoride–*p*-cresol (9:1, v/v for 1 hour at 0°C).
17. NVS3 activity was measured in the serum of the monkeys that received intravenous NVS3 before sporozoite challenge. Twofold serial dilutions of sera were used in an IFAT with air-dried *P. vivax* sporozoites as the target antigen. To determine if NVS3 reacts with epitopes other than AGDR on sporozoites, aliquots of NVS3 at a concentration of 2.5 μg/ml were incubated with varying amounts of the *P. vivax* peptide $(AGDR)_2$ or the unrelated peptide $(QGPGAP)_2$, a peptide from the repeat region of *P. yoelii* CS protein. The antibody-peptide mixtures were then incubated with *P. vivax* sporozoites and evaluated by IFAT to measure the ability of $(AGDR)_2$ to block the binding of NVS3 to sporozoites.
18. VIVAX-1 is a recombinant protein containing approximately 60% of the entire CS protein from the Belem strain of *P. vivax*. It contains the repeat regions $(DRA/_D^AGQPAG)_{20}$ [P. J. Barr *et al.*, *J. Exp. Med.* **165**, 1160 (1987)]. $NS1_{81}V20$ vaccine is a fusion protein from *Escherichia coli* that contains 20 copies of the nonapeptide repeat present in the repeat region of the CS protein and 81 amino acids derived from the nonstructural protein gene of influenza A [D. M. Gordon *et al.*, *Am. J. Trop. Med. Hyg.* **42**, 527 (1990)].
19. *Saimiri* monkey liver fragments were dissociated by collagenase perfusion and plated in 35-mm petri dishes. Equal volumes of serum and sporozoite suspension were mixed and incubated at room temperature for 15 min. The serum-sporozoite mixtures were exposed to the hepatocytes for 2 hours then washed. Seven days after exposure, the monolayers were fixed and schizonts counted microscopically [P. Millet *et al.*, *Am. J. Trop. Med. Hyg.* **38**, 340 (1988)].
20. L. S. Rickman *et al.*, *Clin. Res.* **38**, 352A (1990); C. R. Alving *et al.*, in preparation.
21. The authors note with sadness that Richard L. Beaudoin, our friend and colleague, passed away on 22 May 1990. The authors thank J. M. Carter of the Walter Reed Army Institute of Research (WRAIR) for his invaluable advice on the methods of epitope scanning and T. Hall, also of WRAIR, for generously donating the anti-trypanosoma monoclonal antibody used as a negative control in the passive transfer studies. We thank J. C. Skinner, V. K. Filipski, and C. Morris for their assistance in the challenge studies and M. Leef for performing the IFAT analyses. We also thank I. Bathurst of the Chiron Corporation, Emeryville, CA, for kindly providing VIVAX-1 and M. Gross of SmithKline Beecham for kindly providing $NS1_{81}V20$ for use in this study. Supported by the Naval Medical Research and Development Command work unit nos. 3M-161102BS13AK111 and 3M162770A870AN121 and by U.S. Agency for International Development Participating Agency Service Agreement no. STB-0453.24-P-HZ-2086-06 to the Centers for Disease Control.

13 July 1990; accepted 24 October 1990

Ability of the c-*mos* Product to Associate with and Phosphorylate Tubulin

RENPING ZHOU, MARIANNE OSKARSSON, RICHARD S. PAULES, NICHOLAS SCHULZ, DON CLEVELAND, GEORGE F. VANDE WOUDE

The *mos* proto-oncogene product, pp39^{mos}, is a protein kinase and has been equated with cytostatic factor (CSF), an activity in unfertilized eggs that is thought to be responsible for the arrest of meiosis at metaphase II. The biochemical properties and potential substrates of pp39^{mos} were examined in unfertilized eggs and in transformed cells in order to study how the protein functions both as CSF and in transformation. The pp39^{mos} protein associated with polymers under conditions that favor tubulin oligomerization and was present in an approximately 500-kilodalton "core" complex under conditions that favor depolymerization. β-Tubulin was preferentially coprecipitated in pp39^{mos} immunoprecipitates and was the major phosphorylated product in a pp39^{mos}-dependent immune complex kinase assay. Immunofluorescence analysis of NIH 3T3 cells transformed with *Xenopus* c-*mos* showed that pp39^{mos} colocalizes with tubulin in the spindle during metaphase and in the midbody and asters during telophase. Disruption of microtubules with nocodazole affected tubulin and pp39^{mos} organization in the same way. It therefore appears that pp39^{mos} is a tubulin-associated protein kinase and may thus participate in the modification of microtubules and contribute to the formation of the spindle. This activity expressed during interphase in somatic cells may be responsible for the transforming activity of pp39^{mos}.

THE PROTO-ONCOGENE C-*MOS* IS EXpressed at high levels in the germ cells of vertebrates (*1, 2*). In *Xenopus* and mouse oocytes, the *mos*-encoded protein, pp39^{mos}, is expressed during oocyte maturation and is required for maturation before and after germinal vesicle breakdown (GVBD) (*2–5*). Injection of *mos* RNA into fully grown *Xenopus* oocytes can induce both GVBD and maturation promoting factor (MPF) (*3*), which is composed of cyclin and p34^{cdc2} (*6*). MPF activation is correlated with GVBD, chromosome condensation, and spindle formation (*7–9*). A second activity present in mature oocytes, cytostatic factor (CSF), is thought to be responsible for the arrest of unfertilized eggs at meiotic metaphase II (*10*). Thus, CSF injected into blastomeres of cleaving embryos arrests cell cleavage at metaphase of mitosis (*10–12*), which is a major control point of the cell cycle (*9*). MPF is present at large concentrations in metaphase II oocytes, and it has been proposed that CSF stabilizes MPF (*7, 9, 13, 14*). Recently, pp39^{mos} has been shown to be the active component in CSF (*13*). It is possible to isolate pp39^{mos} from cytosolic extracts by high-speed centrifugation (*13*), which suggests that it is present in a large complex. In addition, the large size of the mitotic spindle in CSF-arrested blastomeres (*11*) and the ability of taxol—a plant diterpene antineoplastic agent that binds to and stabilizes microtubules (*15, 16*)—to arrest cleaving embryos at metaphase (*16*) suggested to us that pp39^{mos} might be associated with tubulin.

We subjected a CSF cytosolic extract pre-

R. Zhou, M. Oskarsson, R. S. Paules, N. Schulz, G. F. Vande Woude, ABL-Basic Research Program, NCI-Frederick Cancer Research and Development Center, Frederick, MD 21702.
D. Cleveland, Department of Biological Chemistry, Johns Hopkins University School of Medicine, Baltimore, MD 21205.

pared from mature oocytes to gel filtration analyses and observed that when extracts were prepared at 2°C, pp39^{mos} eluted as a peak corresponding to a size of ~500 kD (Fig. 1A). However, when this extract was incubated at 37°C for 20 min, which are conditions that favor tubulin polymerization, pp39^{mos} eluted in many fractions (Fig. 1B), which corresponded to molecular sizes much larger than those observed at 2°C (the proteins in fraction 15 and 16 are not *mos*-related).

NIH 3T3 cells transformed by *Xenopus* c-*mos* (c-*mos*^{Xe}) (*3, 17*) express high levels of pp39^{mos} (0.01 to 0.1% of total protein). We examined cytosolic extracts prepared from these cells by gel filtration and found that the size of the pp39^{mos} complex also increased after incubation at 37°C (*18*). In addition, we found that the size of the pp39^{mos} complex was influenced by the protein concentration of the extract (Fig. 2). Gel filtration performed on cytosolic extracts prepared with a protein concentration of ~2 mg/ml, showed pp39^{mos} in size classes of up to >5000 kD (Fig. 2A). However, pp39^{mos} eluted in an ~500-kD peak (Fig. 2B) when the protein concentration of the extract was tenfold lower (~0.2 mg/ml), presumably the result of dissociation of the *mos*-containing complexes.

The conditions—temperature and protein concentration—that affected the size of the pp39^{mos} complex are also conditions that influence tubulin polymerization (*19*). To determine whether the distribution of the pp39^{mos} complex paralleled tubulin distribution, we performed protein immunoblot analysis (*20*) with an antibody to α-tubulin (anti–α-tubulin) on the gel filtration fractions from both the *Xenopus* oocyte and c-*mos*^{Xe}–transformed cell extracts. Tubulin and pp39^{mos} coeluted under conditions that favor the oligomerization of tubulin (Figs. 1B and 2A). Moreover, pp39^{mos} and tubulin also coeluted when the concentrated protein extract from c-*mos*^{Xe}–transformed cells was fractionated by anion-exchange chromatography (Fig. 2C), but they were partially separated when the dilute extract was analyzed in a similar manner (Fig. 2D). It is unlikely that coelution of pp39^{mos} and tubulin after gel filtration and anion-exchange chromatography at a protein concentration of 2 mg/ml are due to nonspecific interactions or protein overloading because other proteins were well separated under these conditions (*18*). Further evidence for a specific pp39^{mos}-tubulin complex is the constant ratio of the two proteins in the high-molecular-mass forms in all of these analyses (Figs. 1B and 2, A and C).

To further analyze the association between pp39^{mos} and tubulin, extracts of [^{35}S]methionine and [^{35}S]cysteine metabolically labeled c-*mos*^{Xe}–transformed NIH 3T3 cells were immunoprecipitated with the *mos* product–specific 5S monoclonal antibody at 2°C. Precipitations were carried out in the presence and absence of a competing synthetic *mos*-encoded peptide (*20*). When a portion of the immune complex was analyzed directly, both pp39^{mos} and a protein with the mobility of tubulin (50 kD) were specifically precipitated (Fig. 3A, lane 1). Neither pp39^{mos} nor the 50-kD protein were precipitated either in the presence of competing peptide (Fig. 3A, lane 2) or from normal 3T3 cells (Fig. 3A, lane 3). To test whether the 50-kD protein was indeed tubulin, the remainder of the pp39^{mos} immune complex was boiled in SDS, adjusted to 1× radioimmunoprecipitation assay (RIPA) buffer, and subjected to precipitation with either anti–α-tubulin or an antibody to β-tubulin (anti–β-tubulin). Both antibodies precipitated a protein with the mobility of tubulin (Fig. 3A, lanes 4 and 5), although anti–β-tubulin precipitated significantly more material. Tubulin was also found to

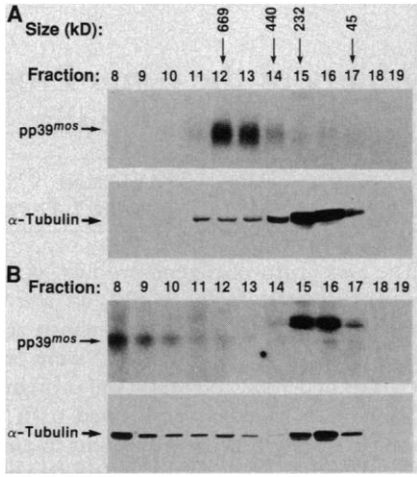

Fig. 1. Gel filtration analysis of extracts from matured *Xenopus* oocytes. Between 500 and 1000 fully grown oocytes (*31*) were collected, treated with progesterone, and labeled in modified Barth solution (MBS) containing progesterone (5 μg/ml) and Translabel {ICN; 75% [^{35}S]methionine and 15% [^{35}S]cysteine (1 mCi/ml)} for 17 hours at 20°C (*13*). Matured oocytes were washed five times with cold CSF buffer [0.25 M sucrose, 0.2 M NaCl, 2.5 mM EGTA, 10 mM sodium phosphate (pH 6.5)] and placed in ultracentrifuge tubes. After excess buffer was removed, the oocytes were centrifuged at 150,000*g* for 1 hour at 2°C, and 200 μl of the cytosolic supernatant (~20 mg of protein per milliliter) were fractionated by gel filtration on a Superose 6 column (Pharmacia). Proteins were eluted in CSF buffer. Half of each 1-ml fraction was immunoprecipitated with the *mos*-product specific 5S antibody (*3*) and analyzed by SDS–polyacrylamide gel electrophoresis (SDS-PAGE) (*32*) (upper panels). Forty microliters of each fraction were analyzed for tubulin by immunoblot analysis (*20*). Tubulin was detected with a monoclonal antibody to α-tubulin (Sigma) and alkaline phosphatase–conjugated goat antiserum to mouse immunoglobulin G (IgG) (Bio-Rad) (lower panels). Ovalbumin (45 kD), catalase (232 kD), ferritin (440 kD), and thyroglobulin (669 kD) were used to calibrate the column for molecular mass. (**A**) Extracts from mature *Xenopus* oocytes were prepared and analyzed at 2°C on a Superose 6 column. The pp39^{mos} protein eluted as a ~500-kD peak, whereas tubulin was predominantly depolymerized and in dimer form. (**B**) The extract prepared as in (A) was incubated at 37°C for 20 min and fractionated at room temperature. The 45-kD doublets in fractions 15 and 16 are probably nonspecific proteins that cross-react with the 5S antibody.

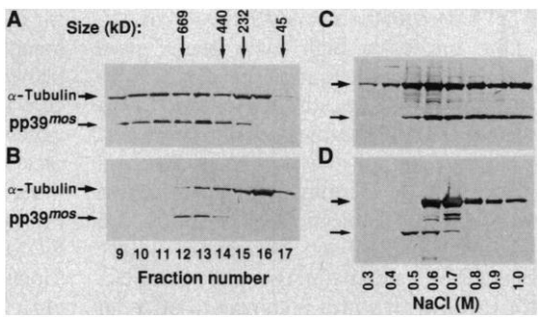

Fig. 2. (**A** and **B**) The influence of protein concentration on the gel filtration elution profile of pp39^{mos} and tubulin in extracts from c-*mos*^{Xe}–transformed NIH 3T3 cells. Either 2 × 10^6 (A) or 2 × 10^5 (B) c-*mos*^{Xe}–transformed cells were rinsed twice with phosphate-buffered saline (PBS), and the cell pellet was suspended in 0.5 ml of lysis buffer [1% NP-40, 150 mM NaCl, 1 mM EDTA, 10 mM sodium phosphate (pH 7.2), 2 mM dithiothreitol (DTT)] with 20 mM leupeptin, 2 mM phenylmethylsulfonyl fluo-ride (PMSF), 10 mM pepstatin, aprotinin (100 units per milliliter)]. The lysate was centrifuged at 100,000*g* for 1 hour, and NaF, $MgSO_4$, β-mercaptoethanol, and adenosine triphosphate (ATP) were added to the supernatant to final concentrations of 10, 10, 10, and 6 mM, respectively. A 200-μl portion of each extract [(A) 2 mg of protein per milliliter; (B) 0.2 mg of protein per milliliter] was fractionated on a Superose 6 column at 2°C as described in the legend to Fig. 1. Proteins in 500 μl of each 1-ml fraction were precipitated by adding 50 μl of 100% trichloroacetic acid and 10 μl of 1% sodium deoxycholate. The precipitate was washed with 100% methanol and analyzed by SDS-PAGE (*32*) and immunoblot analysis (*20*) with either the 5S antibody or the antibody to α-tubulin as described in the legend to Fig. 1. (**C** and **D**) High (2 mg/ml) and low (0.2 mg/ml) concentration protein extracts, respectively, prepared as above, were applied to anion-exchange Mono Q HR5/5 columns (loading capacity of 20 to 50 mg; Pharmacia). Proteins were eluted with a 0.1 to 1.0 M NaCl linear gradient in lysis buffer. Usually <2 mg of total protein were applied in each of these experiments. The fractions were concentrated and analyzed as described in (A).

coprecipitate with pp39^{mos} when antibodies to several other regions of the *mos* product were used in immunoprecipitation experiments (*21*); each of these antibodies showed backgrounds similar to that of lane 3 in Fig. 3A when tested against extracts from nontransformed NIH 3T3 cells. In addition, pp39^{mos} was coprecipitated by both anti–α-tubulin (Fig. 3A, lane 7) and anti–β-tubulin (Fig. 3A, lane 9) from c-*mos*^{Xe}–transformed NIH 3T3 cells but not from control cells (Fig. 3A, lanes 8 and 10). The identification of pp39^{mos} in the tubulin immune complex was confirmed by a second precipitation with the 5S antibody; pp39^{mos} was precipitated from the tubulin immune complex from the transformed cells (Fig. 3A, lane 11) but not from control cells (Fig. 3A, lane 12).

Although anti–β-tubulin precipitated more product in the reprecipitation experiments (Fig. 3A), anti–α-tubulin is more reactive (*22*). Thus, it appears that pp39^{mos} associates preferentially with β-tubulin. This was tested by direct analysis of the ^{35}S-labeled pp39^{mos} immune complex on a gel system that separates α- and β-tubulin (Fig. 3D). Under these conditions, we observed that approximately eight times more β-tubulin was coprecipitated in the pp39^{mos}-tubulin immune complex than α-tubulin (Fig. 3D, lane 1). However, anti–α-tubulin precipitated equal quantities of both α- and β-tubulin from the same extract (Fig. 3D, lane 3), as would be expected because of the formation of α- and β-tubulin heterodimers.

To determine whether tubulin was a substrate for the pp39^{mos} kinase, we immunoprecipitated unlabeled extracts from either c-*mos*^{Xe}–transformed NIH 3T3 cells (Fig. 3B) or unfertilized *Xenopus* eggs (Fig. 3C) with the 5S antibody, and the pp39^{mos} immunoprecipitates were used in in vitro protein kinase reactions. Part of the phosphorylation products were analyzed on SDS-PAGE. The major phosphorylated products had the same electrophoretic mobilities as pp39^{mos} and tubulin. The remainder of the pp39^{mos} kinase reaction products were boiled in SDS, adjusted to 1× RIPA buffer, and precipitated with either 5S or anti-tubulin antibodies. The 5S antibody immunoprecipitates contained pp39^{mos} (Fig. 3, B and C, lanes 3) and a smaller amount of a protein with the same mobility as tubulin (Fig. 3B, lane 3), suggesting that some reformation of the protein complex occurred even after boiling in SDS. When the reprecipitations were performed with anti–α-tubulin or anti–β-tubulin, labeled proteins with the mobility of tubulin were observed (Fig. 3, B and C, lanes 4 and 5). Again, more ^{32}P-labeled tubulin was precipitated with anti–β-tubulin than with anti–α-tubulin.

To exclude the possibility that nonspecific kinases in the pp39^{mos} immune complex were responsible for tubulin phosphorylation, we performed in vitro kinase assays with the product of a *mos* deletion mutant (p28), which lacks the NH_2-terminal adenosine triphosphate (ATP) binding domain

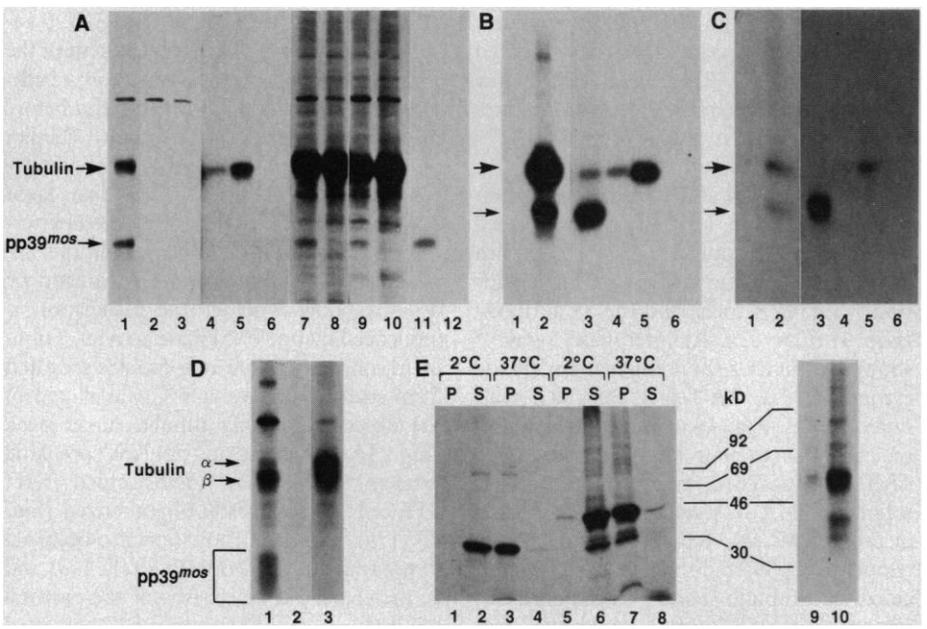

Fig. 3. Tubulin coprecipitates with and is phosphorylated by the pp39^{mos} kinase. (**A**) NIH 3T3 cells transformed by c-*mos*^{Xe} were incubated for 17 hours with Translabel (0.5 mCi/ml) in Dulbecco's modified Eagle's medium (DMEM) containing one-tenth the normal concentrations of methionine and cysteine. A cytosolic extract was prepared as described in the legend to Fig. 2 and subjected to immunoprecipitation in the absence of SDS with the 5S antibody without (lane 1) or with (lane 2) competing peptide (*20*). As an additional control, labeled normal NIH 3T3 cell extract was subjected to immunoprecipitation with the 5S antibody in parallel (lane 3). Extracts containing approximately equal amounts of radioactivity were used in the immune precipitations in lanes 1 to 3. One-fourth of each sample was directly analyzed by SDS-PAGE (lanes 1 to 3). The remainder of the sample analyzed in lane 1 was boiled in 0.5% SDS as described (*33*) and after was adjusted to 1× radioimmunoprecipitation assay (RIPA) buffer, and reprecipitated with either anti–α-tubulin (lane 4), anti–β-tubulin (lane 5), or a nonspecific monoclonal antibody (lane 6). Tubulin was also directly precipitated from the cytosolic extract of c-*mos*^{Xe}–transformed cells (lanes 7 and 9) or normal NIH 3T3 cells (lanes 8 and 10) with anti–α-tubulin (lanes 7 and 8) or anti–β-tubulin (lanes 9 and 10). Half of each of the immune complexes analyzed in lanes 7 and 8 was reprecipitated with the 5S antibody (lanes 11 and 12, respectively). Proteins in different lanes cannot be quantitatively compared because different exposure times were used. (**B**) Cytosolic extracts from unlabeled c-*mos*^{Xe}–transformed NIH 3T3 cells were prepared and immunoprecipitated with the 5S antibody in the presence (lane 1) or absence (lane 2) of competing peptide as in (A). The kinase assay was performed as described (*34*). As in (A), a portion of the reaction mixture was analyzed directly by SDS-PAGE (lanes 1 and 2). The remainder of the pp39^{mos} immunoprecipitate analyzed in lane 2 was boiled in 0.5% SDS, adjusted to 1× RIPA buffer, and analyzed by reprecipitation with the 5S antibody (lane 3), anti–α-tubulin (lane 4), anti–β-tubulin (lane 5), or a control nonspecific monoclonal antibody (lane 6). (**C**) The in vitro kinase assay and reprecipitation were performed with the immune complex of pp39^{mos} from mature *Xenopus* oocytes as described in (B), with cytosolic extracts being prepared as described in the legend to Fig. 1. Lane 1, 5S antibody with competing peptide; lane 2, 5S antibody without competing peptide; lanes 3 to 5, reprecipitation with 5S antibody, anti–α-tubulin and anti–β-tubulin, respectively, from pp39^{mos} immune complex; lane 6, reprecipitation with control monoclonal antibody. (**D**) A cytosolic extract of ^{35}S-labeled c-*mos*^{Xe}–transformed NIH 3T3 cells was prepared as in (A), subjected to immunoprecipitation, fractionated on a 10% polyacrylamide gel at pH 9.3, and analyzed by densitometry (Shimadzu); correction was made for an expected labeling ratio of 1.6:1 for β versus α-tubulin. Lane 1, 5S antibody (*20*); lane 2, 5S antibody with competing peptide; lane 3, anti–α-tubulin. (**E**) Reticulocyte lysate (20 μl) containing p28^{mos} (lanes 1 to 4) or pp39^{mos} (lanes 5 to 8) translated from in vitro–transcribed RNA (*13*) and labeled with [^{35}S]cysteine was mixed with 80 μl of extract (13 mg/ml) from fully grown *Xenopus* oocytes, incubated either at 2°C or 37°C for 1 hour, and centrifuged for 15 min in an Eppendorf microcentrifuge to separate polymerized tubulin from other soluble protein. Equal proportions of the pellet (P) or supernatant (S) fractions were analyzed by SDS-PAGE directly and exposed to x-ray film. In addition, the unlabeled in vitro–translated p28^{mos} and pp39^{mos} proteins were mixed with the unlabeled extract from fully grown oocytes at 2°C as above (lanes 9 and 10) and were then immunoprecipitated with the 5S antibody. In vitro kinase assays were performed on the p28^{mos} (lane 9) and pp39^{mos} (lane 10) immune complexes (*34*).

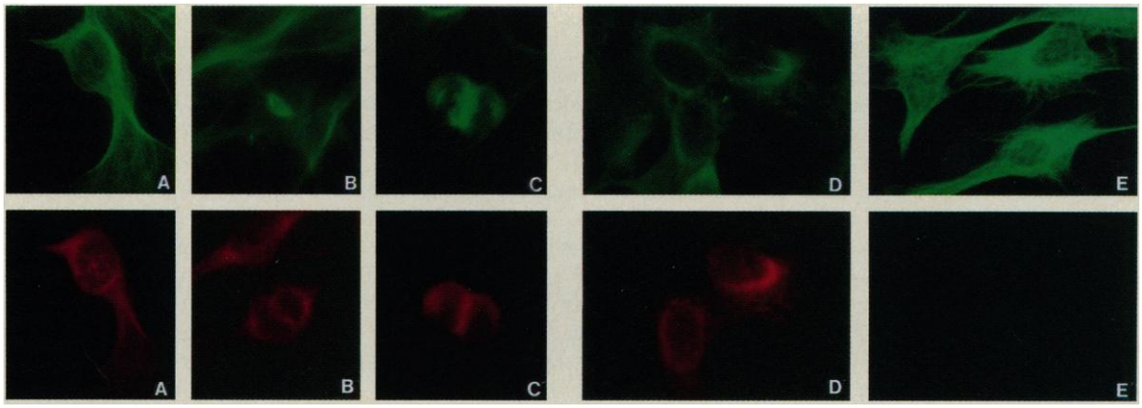

Fig. 4. Tubulin and pp39^{mos} indirect double immunofluorescence study of normal and c-mos^{Xe}–transformed NIH 3T3 cells. Cells were seeded on slides, grown overnight, and then washed in PBS at room temperature. The cells were fixed in methanol at −20°C for 6 min and extracted with 0.1% Triton X-100 in PBS for 1 min. The slides were incubated with 3% bovine serum albumin and 10% goat serum in PBS for 30 min, to block nonspecific antibody binding, and then sequentially with primary and secondary antibodies for 3 hours each in the same buffer. Tubulin was detected with a rat monoclonal antibody (YL 1/2; Accurate) and fluorescein-conjugated goat antibody to rat IgG (no cross-reactivity with mouse IgG) (**A** to **E**). The pp39^{mos} protein was detected with a combination of the 5S antibody and Texas red–conjugated sheep antibody to mouse IgG (Amersham) (**A′** to **E′**). Cover slips were mounted in Mowiol (Aldrich) and slides were examined and photographed at a magnification of ×800 in a Zeiss Photomicroscope II fluorescence system. (A and A′) Interphase cells; (B and B′) metaphase cells; (C and C′) anaphase cells. (D and D′) Cells were incubated for 2 hours in DMEM medium containing nocodazole (1 μg/ml) at 37°C before immunofluorescent labeling. (E and E′) As a control, normal NIH 3T3 cells were labeled in parallel.

(*23*) and CSF activity (*13*). The p28^{mos} protein also associated with tubulin in a temperature-dependent manner (Fig. 3E) but was inactive in the immune complex kinase assay and did not induce significant tubulin phosphorylation when compared with pp39^{mos} (Fig. 3E). These results show that in cytosolic extracts, tubulin complexes with pp39^{mos} and is a substrate for pp39^{mos} kinase activity in vitro.

To determine whether pp39^{mos} is associated with tubulin in vivo, we performed double immunofluorescence analyses with the YL 1/2 anti-tubulin monoclonal antibody (Fig. 4, A to E) and the 5S antibody (Fig. 4, A′ to E′). At interphase, pp39^{mos} showed a punctate staining pattern in the cytoplasm (Fig. 4A′) that coincided with microtubules (Fig. 4A). The punctate staining was also evident in the nucleus (Fig. 4A′). At metaphase, as defined by tubulin staining (Fig. 4B), some pp39^{mos} was found in the mitotic spindle (Fig. 4B′). At early telophase, pp39^{mos} distribution again coincided with tubulin staining in the midbody region (Fig. 4C) as well as in the aster region of each daughter cell. To further study the association of pp39^{mos} with microtubules, we treated the transformed cells with nocodazole to disrupt microtubules, and stained the cells with the YL 1/2 (Fig. 4D) and 5S (Fig. 4D′) antibodies. The microtubules in these cells were disrupted and pp39^{mos} formed aggregates and appeared disorganized compared with untreated cells. Furthermore, depolymerized tubulin and pp39^{mos} showed identical distributions. Normal NIH 3T3 cells stained with the YL 1/2 antibody (Fig. 4E) but not with the 5S antibody (Fig. 4E′). We conclude that pp39^{mos} is associated with microtubules and the spindle in vivo.

We have shown that pp39^{mos} associates with tubulin in vivo and in vitro. Because the pp39^{mos}-tubulin complex is immunoprecipitated from oocyte extracts prepared and maintained at 2°C (Figs. 1A and 3C), β-tubulin is most likely to be a component of the ~500-kD complex. We do not know whether pp39^{mos} associates with β-tubulin before formation of tubulin dimers or whether pp39^{mos} dissociates α- from β-tubulin under conditions (for example, 2°C) that favor tubulin depolymerization. We have not performed these analyses under conditions appropriate for tubulin polymerization and we do not know whether the association is influenced by pp39^{mos} kinase activity. Tubulin in concentrated protein extracts prepared from mature oocytes at 2°C was eluted in the expected 100-kD tubulin dimer peak (Fig. 1A), whereas in similarly prepared extracts from c-mos^{Xe}–transformed NIH 3T3 cells it was mostly oligomerized (Fig. 2A) (*18*). Oligomer formation also occurred in nontransformed NIH 3T3 cells (*18*) and is, therefore, a characteristic of the parental cell line.

Mouse oocytes in which maturation was blocked by depletion of *mos* product showed a dramatic arrest of microtubule-dependent cytoplasmic organelle transport (*4*). Because pp39^{mos} is the active component of CSF (*13*) and is complexed with tubulin, our results provide direct experimental support for the view that CSF might function through modification of microtubules, as was first suggested by Meyerhof and Masui (*11*). We also note that the antineoplastic drug taxol mimics *mos* function, which raises the possibility of a connection between drug specificity and oncogene function.

The kinetics of the appearance and disappearance of the *mos* product in oocytes and fertilized eggs (*3, 13, 20*) parallel spindle formation, metaphase II arrest, and poleward migration of chromosomes during anaphase (*24, 25*). The polymerization of tubulin is a dynamic process (*24*), and we propose that one function of pp39^{mos} may be to influence, directly or indirectly, formation of the spindle and that the arrest of oocytes at metaphase II may involve the stabilization of the spindle by pp39^{mos}. MPF is stabilized by CSF (or pp39^{mos}) (*9, 13, 14*), and recent studies have concluded that pp34^{cdc2} and yeast cyclin are associated with centrosomes and spindle pole bodies during mitosis (*26*). These studies show that the degradation of cyclin and the activation of *cdc2* are dependent on microtubule function (*26*). In yeast, overexpression of α- and β-tubulin results in mitotic arrest, and β-tubulin overexpression has a more profound effect than α-tubulin (*27*). Thus, stabilization of the spindle during metaphase II of meiosis by pp39^{mos} (*13, 20*) could affect centrosome properties and the associated pp34^{cdc2} and cyclin to prevent MPF inactivation. It has also been shown that the *mos* product phosphorylates cyclin in vitro (*28*), and our results do not exclude the possibility that cyclin is a substrate of the pp39^{mos} kinase.

The toxicity of Moloney murine sarcoma virus during acute infection of somatic cells (*29*) is associated with high levels of expression of the v-*mos* product (*30*) and is likely to result from CSF activity (*13*). However, a major question is how low constitutive levels of the v-*mos* or c-*mos* products induce the expression of a transformed phenotype. We have suggested that some properties of transformed cells may be due to the expression of mitotic activities during interphase (*2, 3, 13*). For example, morphological al-

terations, such as mitotic cell rounding, could be responsible for the altered morphology of the transformed cell if they are expressed during interphase. We propose that concentrations of pp39^{mos} that do not prevent cell proliferation or induce CSF "toxicity" can constitutively modify interphase microtubules and could, therefore, induce the transformed phenotype.

REFERENCES AND NOTES

1. F. Propst and G. F. Vande Woude, *Nature* **315**, 516 (1985); G. L. Mutter and D. J. Wolgemuth, *Proc. Natl. Acad. Sci. U.S.A.* **84**, 5301 (1987); D. S. Goldman *et al., ibid.*, p. 4509.
2. N. Sagata, M. Oskarsson, T. Copeland, J. Brumbaugh, G. F. Vande Woude, *Nature* **335**, 519 (1988).
3. N. Sagata, I. Daar, M. Oskarsson, S. D. Showalter, G. F. Vande Woude, *Science* **245**, 643 (1989).
4. R. S. Paules, R. Buccione, R. C. Moschel, G. F. Vande Woude, J. J. Eppig, *Proc. Natl. Acad. Sci. U.S.A.* **86**, 5395 (1989).
5. S. J. O'Keefe *et al., ibid.*, p. 7038.
6. J. Gautier, C. Norbury, M. Lohka, P. Nurse, J. Maller, *Cell* **54**, 433 (1988); G. Draetta *et al., ibid.* **56**, 829 (1989); J. Gautier *et al., ibid.* **60**, 487 (1990).
7. M. J. Lohka and J. L. Maller, *J. Cell Biol.* **101**, 518 (1985).
8. A. W. Murray and M. W. Kirschner, *Nature* **339**, 275 (1989).
9. ———, *Science* **246**, 614 (1989).
10. Y. Masui and C. Markert, *J. Exp. Zool.* **177**, 129 (1971).
11. P. G. Meyerhof and Y. Masui, *Dev. Biol.* **61**, 214 (1977).
12. E. K. Shibuya and Y. Masui, *ibid.* **129**, 253 (1988).
13. N. Sagata, N. Watanabe, G. F. Vande Woude, Y. Ikawa, *Nature* **342**, 512 (1989).
14. A. W. Murray, M. J. Solomon, M. W. Kirschner, *ibid.* **339**, 280 (1989).
15. P. B. Schiff, J. Fant, S. B. Horwitz, *ibid.* **277**, 665 (1979).
16. S. R. Heidemann and P. T. Gallas, *Dev. Biol.* **80**, 489 (1980).
17. R. S. Freeman *et al., Proc. Natl. Acad. Sci. U.S.A.* **86**, 5805 (1989); N. Yew, M. Oskarsson, I. Daar, D. G. Blair, G. F. Vande Woude, *Mol. Cell. Biol.*, in press.
18. Cytosolic extracts (~2 mg of protein per milliliter) of c-*mos*^{Xe}–transformed cells were prepared as described (Fig. 2), and portions were subjected, after incubation at 37° or 2°C for 20 min, to either gel filtration or anion-exchange chromatography. The fractions were analyzed by SDS–polyacrylamide gel electrophoresis (SDS-PAGE) and Coomassie blue staining for total protein and by protein immunoblotting for pp39^{mos} and tubulin. Most pp39^{mos} and tubulin were recovered in the void volume of the gel filtration column after incubation at 37°C, whereas they were more evenly distributed over different fractions after incubation at 2°C (Fig. 2A). Under conditions in which pp39^{mos} and tubulin coeluted as oligomers, or after anion-exchange chromatography, other cellular proteins were well separated. When cytosolic extracts (~2 mg/ml) from control NIH 3T3 cells were analyzed at 2°C, tubulin was present in many fractions, similar to the profile in Fig. 2A.
19. R. C. Weisenberg, *Science* **177**, 1104 (1972); M. L. Shelanski, F. Gaskin, C. R. Cantor, *Proc. Natl. Acad. Sci. U.S.A.* **70**, 765 (1973); G. G. Borisy, J. M. Marcum, J. B. Olmsted, D. B. Murphy, K. A. Johnson, *Ann. N.Y. Acad. Sci.* **253**, 107 (1975).
20. N. Watanabe, G. F. Vande Woude, Y. Ikawa, N. Sagata, *Nature* **342**, 505 (1989).
21. A goat antibody (Ap335) to the pp39^{mos} peptide VERFLPRDLSPSIDLRPC present near the NH_2-terminus and a rabbit antibody (Ap232) to AEQLLERLEQECAM near the COOH-terminus also coprecipitated tubulin with pp39^{mos} specifically from the cytosol of c-*mos*^{Xe}–transformed cells. Furthermore, tubulin was heavily phosphorylated in in vitro immunocomplex kinase assays with these antibodies. (Abbreviations for the amino acid residues are A, Ala; C, Cys; D, Asp; E, Glu; F, Phe; G, Gly; H, His; I, Ile; K, Lys; L, Leu; M, Met; N, Asn; P, Pro; Q, Gln; R, Arg; S, Ser; T, Thr; V, Val; W, Trp; and Y, Tyr.)
22. The anti–α-tubulin monoclonal antibody (DM 1A; Sigma) precipitated three times more tubulin than the anti–β-tubulin monoclonal antibody (Amersham) when equal dilutions (1:100) were used in immune precipitations of ^{35}S-labeled cytosolic extracts from either c-*mos*^{Xe}–transformed cells or control NIH 3T3 cells. (Correction was made for the associated β-tubulin in the anti–α-tubulin immune complex. Anti–β-tubulin precipitated only β-tubulin.)
23. R. S. Paules *et al., Oncogene* **3**, 59 (1988).
24. M. W. Kirschner and T. Mitchison, *Cell* **45**, 329 (1986).
25. D. E. Koshland, T. J. Mitchison, M. W. Kirschner, *Nature* **331**, 499 (1988).
26. E. Bailly, M. Doree, P. Nurse, M. Bornens, *EMBO J.* **8**, 3985 (1989); C. E. Alfa *et al., Nature* **347**, 680 (1990).
27. D. Burke *et al., Mol. Cell. Biol.* **9**, 1049 (1989); W. Katz *et al., ibid.* **10**, 5286 (1990); B. Weinstein and F. Soloman, *ibid.*, p. 5295.
28. L. M. Roy *et al., Cell* **61**, 825 (1990).
29. P. J. Fischinger and D. K. Haapala, *J. Gen. Virol.* **13**, 203 (1971).
30. J. Papkoff, E. A. Nigg, T. Hunter, *Cell* **33**, 161 (1983).
31. J. N. Dumont, *J. Morphol.* **136**, 153 (1972).
32. U. K. Laemmli, *Nature* **227**, 680 (1970).
33. F. P. Rauscher III *et al., Science* **240**, 1010 (1988).
34. Immunoprecipitation was performed as follows: Extracts prepared as described (legends to Figs. 1 and 2) were incubated with the 5S antibody (1:100 dilution) for 3 hours at 2°C. The samples were then centrifuged in an Eppendorf microcentrifuge for 15 min at 2°C to remove protein aggregates. Protein A–Sepharose (BRL) was then added to a final concentration of 1% and the samples were incubated at 2°C for 30 min. The protein A immune complex was collected by centrifugation in an Eppendorf centrifuge for 15 s at 2°C and washed six times with lysis buffer [1% NP-40, 150 mM NaCl, 1 mM EDTA, 10 mM sodium phosphate (pH 7.2)]. The immune complex was then analyzed by SDS-PAGE or assayed for kinase activity as described below. For the in vitro kinase assay, the washed protein A immune complex was resuspended in 50 μl of kinase buffer A [0.1% NP-40, 150 mM NaCl, 10 mM sodium phosphate (pH 7.2), 2 mM dithiothreitol (DTT), 1 mM sodium pyrophosphate] [W. S. Kloetzer, S. A. Maxwell, R. H. Arlinghaus, *Virology* **138**, 143 (1984)]. Five microliters of 2 mM Quercetin (in *N,N*-dimethylformamide) were added and the reaction mixture was incubated for 5 min at 0°C. After addition of 50 μl of kinase buffer B {0.1% NP-40, 150 mM NaCl, 10 mM sodium phosphate (pH 7.2), 2 mM DTT, 1 mM sodium pyrophosphate, 15 mM $MnCl_2$, 20 μM ATP, 10 μCi [γ-^{32}P]ATP}, the reaction mixture was incubated at room temperature for 15 min. The reaction was terminated by dilution with lysis buffer. The protein A immune complex was then washed four times with lysis buffer to remove free [γ-^{32}P]ATP and analyzed by SDS-PAGE or by reprecipitation as described in the legend to Fig. 3.

35. We thank J. Brugge, N. Copeland, P. Johnson, S. J. O'Brien, R. Gilden, D. Faletto, N. Wilkie, and I. Daar for critical comments and helpful discussion; A. Arthur for editorial comment; and L. Summers for preparation of the manuscript. Supported in part by the National Cancer Institute, DHHS, under contract No. NO1-CO-74101 with ABL, Inc.

29 August 1990; accepted 9 November 1990

A68: A Major Subunit of Paired Helical Filaments and Derivatized Forms of Normal Tau

VIRGINIA M.-Y. LEE,* BRIAN J. BALIN, LASZLO OTVOS, JR., JOHN Q. TROJANOWSKI

Putative Alzheimer disease (AD)–specific proteins (A68) were purified to homogeneity and shown to be major subunits of one form of paired helical filaments (PHFs). The amino acid sequence and immunological data indicate that the backbone of A68 is indistinguishable from that of the protein tau (τ), but A68 could be distinguished from normal human τ by the degree to which A68 was phosphorylated and by the specific residues in A68 that served as phosphate acceptors. The larger apparent relative molecular mass (M_r) of A68, compared to normal human τ, was attributed to abnormal phosphorylation of A68 because enzymatic dephosphorylation of A68 reduced its M_r to close to that of normal τ. Moreover, the LysSerProVal motif in normal human τ appeared to be an abnormal phosphorylation site in A68 because the Ser in this motif was a phosphate acceptor site in A68, but not in normal human τ. Thus, the major subunits of a class of PHFs are A68 proteins and the excessive or inappropriate phosphorylation of normal τ may change its apparent M_r, thus transforming τ into A68.

PHFs ARE THE PRINCIPAL STRUCTURAL elements of AD neurofibrillary tangles (NFTs) (*1*). Although not restricted to AD, the number of NFTs correlates with the severity of dementia in AD (*1*). PHFs also occur in the neurites surrounding amyloid-rich senile plaque (SP) cores, and in neuropil threads (NTs) that represent altered neuronal processes (*1*). Low M_r microtubule-associated proteins (MAPs) known as τ are major constituents of PHFs (*1*). A soluble form of PHFs may be formed from τ (*2*). Although other neu-

V. M.-Y. Lee, B. J. Balin, J. Q. Trojanowski, Department of Pathology and Laboratory Medicine, University of Pennsylvania School of Medicine, Philadelphia, PA 19104.

L. Otvos, Jr., Wistar Institute of Anatomy and Biology, Philadelphia, PA 19104.